



The Compact Muon Solenoid Experiment  
**Conference Report**

Mailing address: CMS CERN, CH-1211 GENEVA 23, Switzerland



05 February 2020 (v4, 26 February 2020)

# Radiation Resistant Innovative 3D Pixel Sensors for the CMS Upgrade at the High Luminosity LHC

Marco Meschini for the CMS Collaboration

## Abstract

An extensive R&D program aiming at radiation hard, small pitch, 3D pixel sensors has been put in place between Istituto Nazionale di Fisica Nucleare (INFN, Italy) and FBK Foundry (Trento, Italy). The CMS experiment is supporting the R&D in the scope of the Inner Tracker upgrade for the High Luminosity phase of the CERN Large Hadron Collider (HL-LHC). In the HL-LHC the Inner Tracker will have to withstand an integrated fluence up to  $2.3 \times 10^{16} \text{ n}_{\text{eq}}/\text{cm}^2$ . A small number of 3D sensors were interconnected with the RD53A readout chip, which is the first prototype of 65 nm CMOS pixel readout chip designed for the HL-LHC pixel trackers. In this paper results obtained in beam tests before and after irradiation are reported. Irradiation of a single chip module was performed up to a maximum equivalent fluence of about  $1 \times 10^{16} \text{ n}_{\text{eq}}/\text{cm}^2$ . Analysis of the collected data shows excellent performance: spatial resolution in not irradiated (fresh) sensors is about 3 to 5  $\mu\text{m}$  depending on the pixel pitch. Hit detection efficiencies are close to 99% measured both before and after the above mentioned irradiation fluence.

Presented at *HSTD12 12th International Hiroshima Symposium on the Development and Application of Semiconductor Tracking Detectors (HSTD12)*

# Radiation Resistant Innovative 3D Pixel Sensors for the CMS Upgrade at the High Luminosity LHC

M. Meschini<sup>a,\*</sup>, A. Cassese<sup>a</sup>, R. Ceccarelli<sup>a,b</sup>, L. Viliani<sup>a,b</sup>, M. Dinardo<sup>c,d</sup>, S. Gennai<sup>c</sup>, D. Zuolo<sup>c,d</sup>, A. Messineo<sup>j,k</sup>, S. Parolia<sup>j,k</sup>, A. Ebrahimi<sup>f</sup>, D. Pitzl<sup>g</sup>, G. Steinbrück<sup>f</sup>, G. F. Dalla Betta<sup>e,h</sup>, R. Mendicino<sup>e,h</sup>, G. Alimonti<sup>l</sup>, C. Gemme<sup>i</sup>, M. Boscardin<sup>m,h</sup>, S. Ronchin<sup>m</sup>

<sup>a</sup>*INFN Sezione di Firenze, Sesto Fiorentino, Italy*

<sup>b</sup>*Università di Firenze, Dipartimento di Fisica, Firenze, Italy*

<sup>c</sup>*INFN Sezione di Milano Bicocca, Milano, Italy*

<sup>d</sup>*Università di Milano Bicocca, Dipartimento di Fisica, Milano, Italy*

<sup>e</sup>*Università di Trento, Dipartimento di Ingegneria Industriale, Trento, Italy*

<sup>f</sup>*University of Hamburg, Hamburg, Germany*

<sup>g</sup>*Deutsches Elektronen-Synchrotron, Hamburg, Germany*

<sup>h</sup>*TIFPA INFN, Trento, Italy*

<sup>i</sup>*INFN Sezione di Genova, Genova, Italy*

<sup>j</sup>*Università di Pisa, Dipartimento di Fisica, Pisa, Italy*

<sup>k</sup>*INFN Sezione di Pisa, Pisa*

<sup>l</sup>*INFN Sezione di Milano, Milano, Italy*

<sup>m</sup>*Fondazione Bruno Kessler FBK, Trento, Italy*

---

## Abstract

An extensive R&D program aiming at radiation hard, small pitch, 3D pixel sensors has been put in place between Istituto Nazionale di Fisica Nucleare (INFN, Italy) and FBK Foundry (Trento, Italy). The CMS experiment is supporting the R&D in the scope of the Inner Tracker upgrade for the High Luminosity phase of the CERN Large Hadron Collider (HL-LHC). In the HL-LHC the Inner Tracker will have to withstand an integrated fluence up to  $2.3 \times 10^{16} \text{ n}_{\text{eq}}/\text{cm}^2$ . A small number of 3D sensors were interconnected with the RD53A readout chip, which is the first prototype of 65 nm CMOS pixel readout chip designed for the HL-LHC pixel trackers. In this paper results obtained in beam tests before and after irradiation are reported. Irradiation of a single chip module was performed up to a maximum equivalent fluence

---

\*Corresponding Author, on behalf of CMS Tracker Group  
*Email address:* marco.meschini@cern.ch (M. Meschini)

of about  $1 \times 10^{16} \text{ n}_{\text{eq}}/\text{cm}^2$ . Analysis of the collected data shows excellent performance: spatial resolution in not irradiated (fresh) sensors is about 3 to 5  $\mu\text{m}$  depending on the pixel pitch. Hit detection efficiencies are close to 99% measured both before and after the above mentioned irradiation fluence.

*Keywords:* Silicon Detectors, Irradiation, High Luminosity LHC, 3D Pixels, Readout Electronics, Radiation Hard Pixel Sensors

---

## 1. Introduction

The CMS Inner Tracker system will go through a complete redesign and upgrade in order to achieve optimal tracking and physics performance during the High Luminosity phase of Large Hadron Collider at CERN [1]. The pixel detectors, with the first layer located at 30 mm from the beam line, have to be working with good charge collection efficiency up to a fluence which is estimated to reach  $2.3 \times 10^{16} \text{ n}_{\text{eq}}/\text{cm}^2$ . To reach this goal a single pixel will have a size of  $50 \times 50 \mu\text{m}^2$  or  $25 \times 100 \mu\text{m}^2$  and the sensor has a small active thickness, presently fixed in CMS to 150  $\mu\text{m}$ . This active thickness was chosen in order to keep both the bias voltage and the power dissipation after irradiation to a manageable level, while at the same time allowing a reasonable amount of charge to be collected thus reaching very high hit detection efficiency after irradiation. The total thickness, including a possible support wafer, should be kept below 275  $\mu\text{m}$ . In the CMS experiment the options on the final cell geometry aspect ratio and pixel type, should it be planar or 3D, are still open. In this report we will discuss the most recent results obtained with 3D pixel sensors produced by FBK interconnected with the RD53A readout chip [2].

## 2. The FBK 3D Pixel Sensors

The 3D sensors in our R&D program [3], are developed and fabricated in the framework of INFN and FBK collaboration activity [4]. The substrates are p-type Si-Si Direct Bond Wafers (DBW), with a support wafer made of 500  $\mu\text{m}$  thick, less than 1 Ohm cm resistivity, Czochralski (CZ) silicon. The columnar electrodes are implanted on a Float Zone (FZ), high resistivity ( $>3000 \text{ Ohm cm}$ ), 130  $\mu\text{m}$  or 150  $\mu\text{m}$  thick wafer. The columns of both  $p^+$  and  $n^+$  types are etched by Deep Reactive Ion Etching (DRIE) in the FZ wafer using a top-side only process, before being doped. The Ohmic

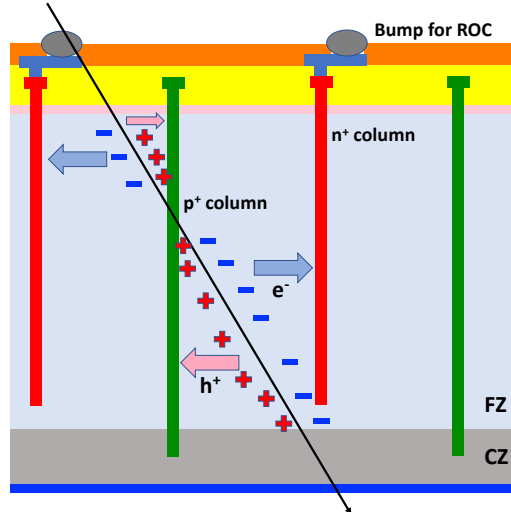


Figure 1: Sketch of a 3D columnar sensor, not to scale;  $n^+$  junction columns are in red,  $p^+$  ohmic columns, reaching the low resistivity CZ support wafer where the reverse bias voltage is applied, are in green.

$p^+$  columns reach the low resistivity layer in the support wafer, where the reverse bias voltage is applied, while junction  $n^+$  columns are optimised to have a length which is on average about  $20\ \mu\text{m}$  shorter than the FZ wafer thickness. The column diameter is about  $5\ \mu\text{m}$  for both types. Two different pixel cell geometries have been implemented:  $50 \times 50\ \mu\text{m}^2$  and  $25 \times 100\ \mu\text{m}^2$ . Metal bump pads for the readout chip are connected to the junction columns via dedicated metal routing, which requires special attention in the case of rectangular pixel cell design because the RD53A readout chip (ROC) has a square  $50 \times 50\ \mu\text{m}^2$  bump pad pitch. A temporary metal layer is used for current voltage (I-V) measurements (both in reverse and forward biasing) at FBK premises to identify defective sensors; the temporary metal is removed before shipping the wafer to the bump-bonding company. In 3D columnar pixel sensors, the charge carriers released by an ionising particle traversing the sensitive volume, have to travel distances of at most  $35\ \mu\text{m}$ , for a  $50 \times 50\ \mu\text{m}^2$  pixel cell (or  $50\ \mu\text{m}$  for a  $25 \times 100\ \mu\text{m}^2$ ) to reach the central collecting electrode; a 3D columnar sensor, showing the charge drifting directions, is schematically shown in Fig. 1. The inter-electrode distance also determines the bias voltage needed to fully deplete the active volume for a given silicon bulk resistivity. This distance is usually, as in the present

case, much shorter than the sensor thickness, which is the basic parameter determining the amount of released charge. In addition to that, after irradiation to the fluences foreseen for the HL-LHC, the radiation damage greatly reduces the effective drift distance of charge carriers because of charge trapping. In 3D pixels the above mentioned short inter-electrode distance and the lower operational bias voltage give an important advantage over the standard planar pixel sensors both before and after irradiation.

### 2.1. The 3D Pixel Modules for the Test Beam

The results reported in this paper come from four single-chip assemblies, also called "modules" in the following. They originate from two different FBK production batches: one  $25 \times 100 \mu\text{m}^2$  and two  $50 \times 50 \mu\text{m}^2$  sensors were made in 2017 with a Mask Aligner batch (MA), one  $50 \times 50 \mu\text{m}^2$  was made in 2019 with a Stepper batch (ST). Mask Aligner and Stepper (Step-and-repeat

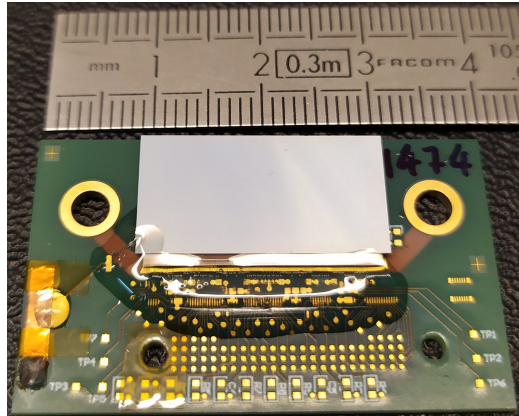


Figure 2: Sensor and RD53A assembly (flip-chip) glued and wire-bonded onto a Rice irradiation card. Wire bonds are encapsulated with silicone elastomer to be protected. The light-gray upper surface is the metalised sensor back-side, where HV bias wire-bonds are connected in the lower left corner.

exposure) are two different photolithographic technologies used in silicon foundries; the Stepper has a higher, sub- $\mu\text{m}$ , precision but it is less flexible with respect to Mask Aligner. In case it is needed to have different cell and sensor designs on the same wafer layout, they can be then patterned in one go on the full wafer by the Mask Aligner. The active thickness of the MA sensors is  $130 \mu\text{m}$ , while for the ST sensor it is  $150 \mu\text{m}$ . The depletion voltage is lower than  $5 \text{ V}$  for all these 3D sensors. The MA sensors were bump-bonded (with

Sn-Ag bumps) to the ROC at Fraunhofer-Institut IZM (Berlin, Germany); the ST sensor was bump-bonded (with Indium bumps) at Leonardo Company (Rome, Italy). The flip-chip assemblies were glued on a printed circuit board specifically designed for test beams and proton irradiations, called the Rice card (designed by the CMS group of Rice University, Houston, TX), and then wire-bonded in INFN Firenze laboratory. The Rice card, shown in Fig. 2, is a very lightweight PCB; the region below the flip-chip is free from material to avoid multiple scattering on the test beam and to minimize the activation under irradiation. The card is connected to an adapter card in order to allow readout by the DAQ system both in lab or at the test beam. One of the 3D  $50 \times 50 \mu\text{m}^2$  MA modules was irradiated at the CERN IRRAD facility in 2018 in a high intensity 24 GeV proton beam to an estimated fluence of  $1 \times 10^{16} \text{ n}_{\text{eq}}/\text{cm}^2$ . This fluence in the IRRAD beam corresponds to a TID (Total Ionising Dose) of about 6 MGy: this is the dose that has to be taken into account for the radiation damage of RD53A readout chip. The IRRAD proton beam has a FWHM of 12 mm in  $x$  and  $y$  directions. The module was mounted with a turn angle of  $55^\circ$  with respect to the beam direction to achieve a more uniform irradiation. All results presented in this paper were obtained with the Linear front-end of RD53A, which is located in the central region of the ROC and is 136 columns wide (6.8 mm), from column 128 to 263 [2].

### 3. Test Beam and Pixel Modules at DESY

The pixel modules were tested at the DESY (Deutsches Elektronen-Synchrotron) Test Beam Facility, in the TB21 area selecting an electron (and positron) beam of 5.2 GeV momentum. The test beam area is equipped with a EUDET beam telescope which allows tracking the beam particles [5]. The telescope is composed of two arms, each of them made of three planes of monolithic active pixel silicon sensors. The Device Under Test (DUT) is placed between the two arms, called upstream and downstream with respect to the beam direction. Two scintillators, whose coincidence signals are used to trigger the DAQ sequence, are placed in front of the first telescope plane, giving a geometrical window of approximately  $10 \text{ mm} \times 10 \text{ mm}$  centered on the electron beam. In order to have a timing reference to correctly reconstruct tracks in the telescope and in the DUT, a pixel module of the type presently in use in the CMS Tracker [6] is placed upstream in front of the first scintillator. The irradiated module was installed inside a cooling box,

keeping the sensor at a low and constant temperature in order to reduce the HV bias current. The cooling box is made of aluminium, thermally insulated, with a cut-out entry window for the incoming electron beam. Inside the

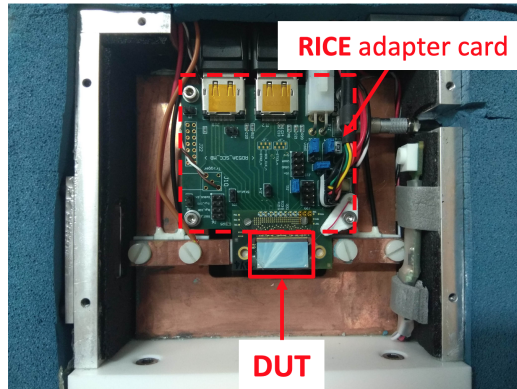


Figure 3: The irradiated  $50 \times 50 \mu\text{m}^2$  module connected to the Rice adapter card and mounted inside the cooling box.

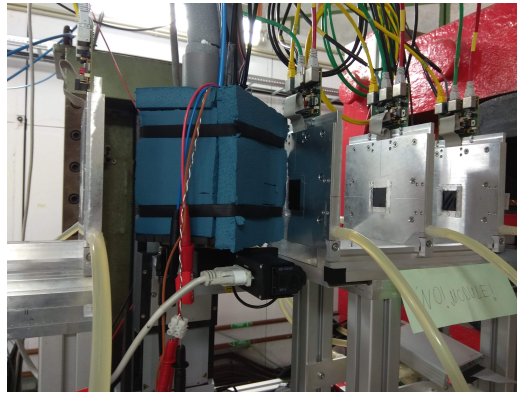


Figure 4: The cooling box on the beam line housing the irradiated module during an angular scan data taking.

box, the downstream face of the DUT was in contact, through a thermally conductive paste, with a thin copper bar, which was kept cold (temperature about  $-27^\circ\text{C}$ ) by two Peltier cells, cooled by an external chiller. The irradiated tested module, mounted in the cooling box, is shown in Fig. 3. The non-irradiated modules were tested in free air, as due to low leakage current no cooling was needed. The cold box can have some impact on the final

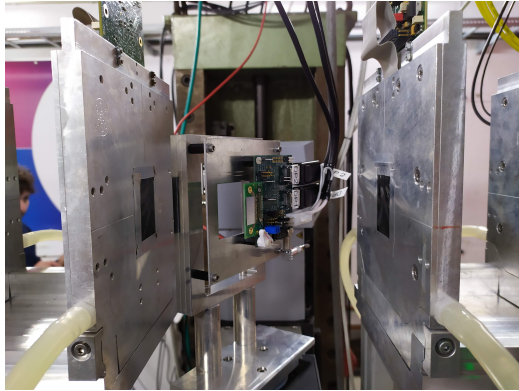


Figure 5: The  $25 \times 100 \mu\text{m}^2$  module mounted on the beam line for the angular scan along the  $25 \mu\text{m}$  pitch coordinate.

achievable track resolution, because of the multiple scattering of the electron beam in the insulating material in front of the module and the metal structure downstream. Thus we chose to take data without the box whenever possible. All the DUTs were mounted on a moveable precision stage which also allowed to turn them with respect to the beam axis and take data at different beam incidence angles. The two configurations for a DUT with and without the cooling box in the beam are shown in Figs. 4 and 5.

### *3.1. Data Taking and Results for Non-Irradiated Modules*

The non-irradiated modules were tuned to about  $900 e^-$  threshold and then tested at two bias voltages: 6 V (which was the minimum stable voltage value provided by the power supply) and 30 V. All modules had hit efficiencies greater than 99% for orthogonally incident tracks, already at very low bias voltage. The measured bias currents are reported in table 1. The stepper module had a bias current much higher than it was when measured on sensor wafer (before dicing and flip-chipping). However even with the higher bias current the module was perfectly working without any impact on performance even in overnight runs of over 25 M collected triggers. The reason for taking data with high statistics and high bias voltage was that we also wanted to prove that 3D sensors can be safely operated with a large margin with respect to the depletion voltage. This could eventually be needed because the upgraded CMS pixel detector will be powered according to a serial powering scheme with up to eight modules in a serial chain. An effect of the serial powering, together with a common HV bias line, is that the HV bias



Table 1: 3D modules bias voltages, currents and efficiencies. The sensor temperature was around 45 °C.

3D Type and Cell Size	Voltage [V]	Current [nA]	Efficiency
MA 50x50	6	150	>99%
MA 50x50	30	250	>99%
MA 25x100	6	130	>99%
MA 25x100	30	190	>99%
ST 50x50	6	6500	>99%
ST 50x50	30	16500	>99%

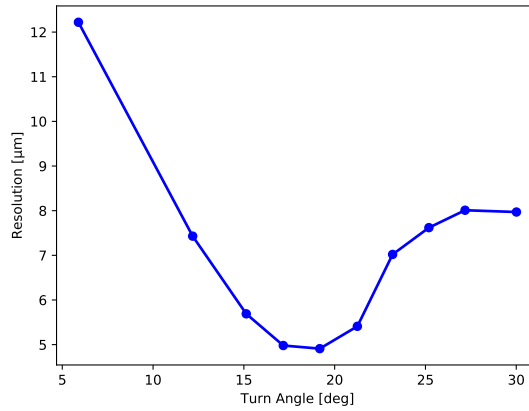


Figure 6: Resolution vs. turn angle for the 50 μm pitch sensor.

voltage drop between the last and the first module in the chain will be 2 V (maximum) per module times the number of modules in the same HV chain. We showed that the 3D modules can be operated at 30 V bias with a 1.5 safety factor with respect to the maximum foreseen bias voltage difference of 16 V bias between modules in the same chain.

In order to evaluate the spatial resolution of the 3D modules, we took data at different turn angles up to 30° with respect to the beam, using the rotating precision stage. Particularly interesting was measuring the 25 × 100 μm<sup>2</sup> pitch module resolution along the 25 μm pitch coordinate, a measurement not yet done, to our knowledge, on this kind of 3D pixel sensors. The spatial resolu-

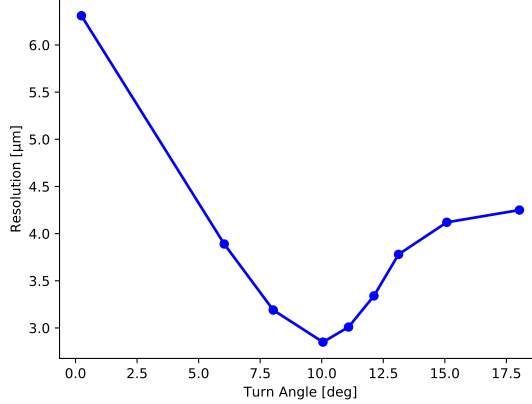


Figure 7: Resolution vs. turn angle for the  $25 \times 100 \mu\text{m}^2$  along the  $25 \mu\text{m}$  pitch coordinate.

tion  $\text{Res}_{\text{DUT}}$  is estimated by the  $\sigma$  obtained fitting the Student’s  $t$ -distribution of the track residuals on the DUT after subtracting the telescope resolution  $\text{Res}_{\text{tele}}$  in quadrature.  $\text{Res}_{\text{tele}}$  goes from  $3.8$  to  $6.2 \mu\text{m}$  depending on the telescope configuration. The angular scans were made at  $30 \text{ V}$  bias for the two MA modules, and the results are plotted in Figs. 6 and 7. There was not enough beam time to make the angular scan on the ST  $150 \mu\text{m}$  thick sensor. No selection cuts of the hit cluster size on the DUT were applied to obtain these distributions. The minimum in the resolution plot is reached for the angle at which a track is crossing two adjacent pixels. This angle is given by  $\tan^{-1}(\text{pitch}/\text{active\_thickness})$ , which for a thickness of  $130 \mu\text{m}$  results in  $21^\circ$  for  $50 \mu\text{m}$  pitch, and  $11^\circ$  for  $25 \mu\text{m}$  pitch; these angles are compatible with the ones where the resolution distributions have a minimum. The best resolutions obtained are  $5 \mu\text{m}$  for  $50 \mu\text{m}$  pitch and slightly better than  $3 \mu\text{m}$  for  $25 \mu\text{m}$  pitch.

### 3.2. Data Taking and Results for the Irradiated Module

In order to take good quality data, the 3D  $50 \times 50 \mu\text{m}^2$  irradiated module was tuned in the cooling box, at low temperature, to a threshold of about  $1150 e^-$ . We performed a bias voltage scan, and the hit efficiency was measured at each point. The maximum effective bias voltage, subtracting the drop on the HV limiting series resistors, was  $146 \text{ V}$  with a bias current of  $120 \mu\text{A}$  at  $-27^\circ\text{C}$ . The hit efficiency curve is shown in Fig. 8. The hit efficiency reaches a “plateau” around  $110 \text{ V}$ , and has a maximum value of

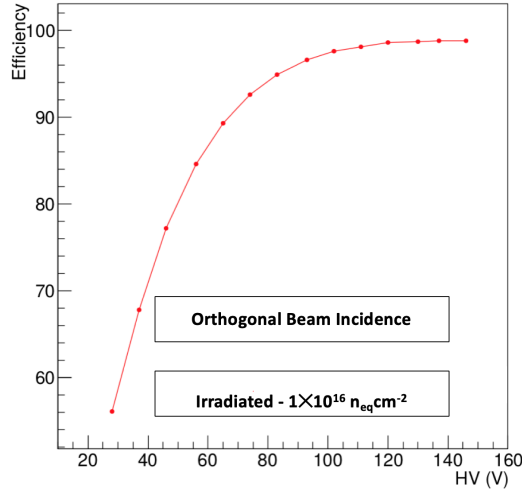


Figure 8: Hit efficiency vs. bias voltage for the irradiated 3D 50  $\mu\text{m}$  pitch module.

98.8% at 146 V. The power dissipation of the sensor is below  $9\text{ mW}/\text{cm}^2$ . Since we were aware that the fluence received by the module in IRRAD was not very homogenous, we performed some cross checks to verify the impact of non-uniformity on the module efficiency. The non-uniformity of the irradiation on the module can be seen by measuring the hit efficiency at a bias voltage which is suitable for having almost full efficiency where the received fluence is lower, but which is not enough to get high efficiency in the most irradiated region. The high fluence region is highlighted with a dotted oval in the module efficiency map obtained for 28 V bias reported in Fig. 9. In the data analysis the DUT was then subdivided in six smaller zones, and the hit efficiency recalculated in each region. The results are compatible with the full DUT hit efficiency of 98.8% for bias voltage above 120 V. As an example, the hit efficiencies in the two most irradiated regions are shown in Fig. 10. As in the case of non-irradiated modules, we made an angular scan to estimate the pixel resolution as a function of the turn angle. During the scan we verified that a track angle of  $6^\circ$  is already sufficient to get a hit efficiency greater than 99%. To estimate the spatial resolution we applied a slightly different fitting procedure because the presence of the material introduced on the beam line by the cooling box made it almost impossible to use the extrapolated exit point on the DUT from the three downstream telescope planes. The telescope resolution was extrapolated using the unrotated DUT coordinate and then the final DUT resolution was obtained as in the case

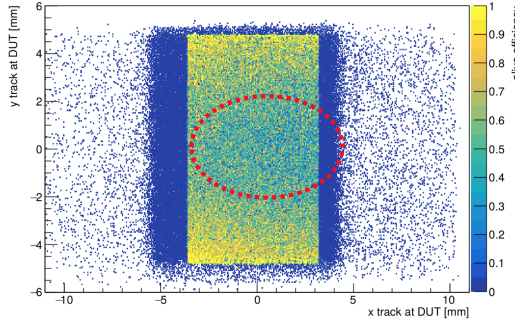


Figure 9: Hit efficiency map for the irradiated 3D 50  $\mu\text{m}$  pitch module at 28 V bias. The higher fluence (lower efficiency) region is indicated with the dotted oval.

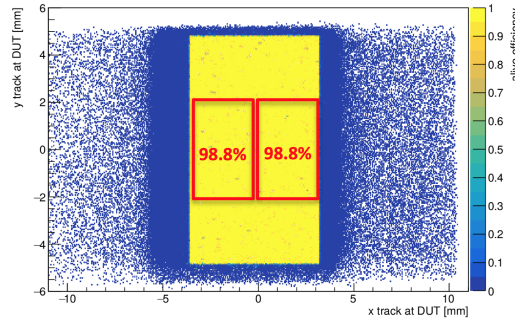


Figure 10: Hit efficiency map in the two most irradiated regions of the 3D module at 146 V bias.

of non-irradiated modules. The spatial resolution as a function of the angle is reported in Fig.11. The best resolution for the 50  $\mu\text{m}$  pitch irradiated module is about 5.7  $\mu\text{m}$ , obtained at  $\simeq 20^\circ$ .

## Conclusions

In this paper we have reported measurements done on FBK 3D pixel sensors bump bonded to the RD53A readout chip for irradiated and non-irradiated single chip modules. The results obtained with the module irradiated to the fluence of  $1 \times 10^{16} \text{ n}_{\text{eq}}/\text{cm}^2$ , corresponding to about half of the fluence expected in the first layer of the upgraded CMS Tracker after 10 years of operation, show that we can reach 99% hit efficiency and a spatial resolution better than 6  $\mu\text{m}$  for a bias voltage of around 150 V. The measurements done with the non-irradiated modules of 130 and 150  $\mu\text{m}$  active thickness are

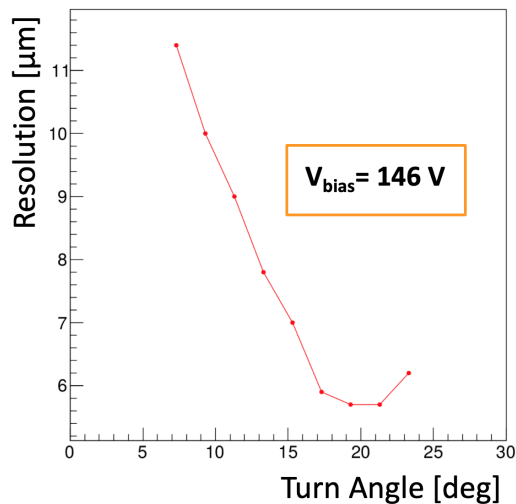


Figure 11: Resolution vs. turn angle for the irradiated 3D 50  $\mu\text{m}$  pitch module.

very satisfactory; the 3D pixel sensors are perfectly efficient already at 6 V bias, and they can be operated without problems at least up to 30 V bias, giving a large margin for the LV serial power operation. We measured for the first time the 3D pixel spatial resolution along the 25  $\mu\text{m}$  pitch direction and we obtained a resolution better than 3  $\mu\text{m}$  for a 10° turn angle for 130  $\mu\text{m}$  sensor thickness. The resolution for the non-irradiated 50  $\mu\text{m}$  pitch sensor is 5  $\mu\text{m}$  for a 20° turn angle. The resolution obtained on the irradiated sensor is around 6  $\mu\text{m}$ . CMS is planning irradiations up to the fluence equivalent to the full HL-LHC lifetime radiation level for the Inner Tracker. Thus new test beam campaigns will be necessary to verify the module performance after such high fluences.

### Acknowledgments

This work was supported by the Italian National Institute for Nuclear Physics (INFN); the project received funding also by EU H2020 AIDA-2020, GA no. 654168.

### References

- [1] K. Klein, et al., The Phase-2 Upgrade of the CMS Tracker, Tech. Rep. CERN-LHCC-2017-009, CMS-TDR-014, CERN, Geneva (June 2017).

URL <http://cds.cern.ch/record/2272264?ln=en>

- [2] M. Garcia-Sciveres, The RD53A Integrated Circuit, Tech. Rep. CERN-RD53-PUB-17-001, CERN, Geneva (Oct 2017).  
URL <https://cds.cern.ch/record/2287593>
- [3] G.-F. Dalla Betta, R. Mendicino, D. Sultan, M. Boscardin, G. Giacomini, S. Ronchin, N. Zorzi, G. Darbo, M. Meschini, A. Messineo, Small pitch 3D devices, PoS Vertex2016 (2017) 028. doi:10.22323/1.287.0028.
- [4] M. Meschini, G. F. Dalla Betta, M. Boscardin, G. Calderini, G. Darbo, G. Giacomini, A. Messineo, S. Ronchin, The INFN-FBK pixel R&D program for HL-LHC, Nucl. Instrum. Meth. A831 (2016) 116–121. doi:10.1016/j.nima.2016.05.009.
- [5] H. Jansen, et al., Performance of the EUDET-type beam telescopes, EPJ Tech. Instrum. 3 (1) (2016) 7. arXiv:1603.09669, doi:10.1140/epjti/s40485-016-0033-2.
- [6] K. Klein, The Phase-1 upgrade of the CMS pixel detector, Nucl. Instrum. Meth. A845 (2017) 101–105. doi:10.1016/j.nima.2016.06.039.